

# Optics Letters

## Silica-based fiber Raman laser at $> 2.4 \mu\text{m}$

HUAWEI JIANG,<sup>1,2</sup> LEI ZHANG,<sup>1,3</sup> AND YAN FENG<sup>1,\*</sup>

<sup>1</sup>Shanghai Key Laboratory of Solid State Laser and Application, and Shanghai Institute of Optics and Fine Mechanics, Chinese Academy of Sciences, Shanghai 201800, China

<sup>2</sup>University of the Chinese Academy of Sciences, Beijing 100049, China

<sup>3</sup>e-mail: zhangl@siom.ac.cn

\*Corresponding author: feng@siom.ac.cn

Received 23 April 2015; revised 9 June 2015; accepted 16 June 2015; posted 19 June 2015 (Doc. ID 239618); published 3 July 2015

**Raman laser generation at the long wavelength transmission edge of silica fiber is explored. Numerical simulation reveals that high efficiency 2nd Stokes Raman laser operation around  $2.5 \mu\text{m}$  is feasible with highly Ge-doped silica fiber as the gain medium and pulsed  $2\text{-}\mu\text{m}$  fiber laser as the pump source. Based on the spontaneous cascaded Raman amplification process,  $0.30\text{-W}$  laser at  $2.43 \mu\text{m}$  is obtained with an optical efficiency of  $16.5\%$  pumped at  $2008 \text{ nm}$ . And  $0.15\text{-W}$  laser at  $2.48 \mu\text{m}$  is achieved with an optical efficiency of  $7.9\%$  pumped at  $2040 \text{ nm}$ . To the best of our knowledge, the results represent the longest wavelength operation of silica-based fiber laser.** © 2015 Optical Society of America

**OCIS codes:** (140.3510) Lasers, fiber; (140.3280) Laser amplifiers; (140.3550) Lasers, Raman; (140.3070) Infrared and far-infrared lasers.

<http://dx.doi.org/10.1364/OL.40.003249>

In recent years, fiber lasers operating at mid-infrared spectral band drew lots of attention due to a large number of applications including LIDAR, gas sensing, and optical communication. Optical fibers made by soft glasses, such as fluoride and chalcogenide, are candidates as gain media for mid-infrared laser generation because they have low phonon energy and are transparent at mid-infrared [1].  $2.85\text{-}$ ,  $3.22\text{-}$ , and  $3.9\text{-}\mu\text{m}$  emissions were obtained from  $\text{Ho}^{3+}$ -doped ZBLAN fiber lasers [2–4].  $2.8\text{-}$  and  $3.5\text{-}\mu\text{m}$  emissions from  $\text{Er}^{3+}$ -doped ZBLAN fiber lasers were also reported [5–7]. Except for RE-doped fiber lasers, Raman fiber lasers or amplifiers are an alternative way to generate a mid-infrared fiber laser, which have the additional advantage of wider wavelength tunability.  $3.7\text{-W}$  fluoride glass Raman fiber laser operating at  $2231 \text{ nm}$  has been reported [8]. A single-mode  $\text{As}_2\text{S}_3$  cascaded Raman fiber laser emitting at  $3.77 \mu\text{m}$  was demonstrated based on nested Fabry–Perot cavities formed by two pairs of FBGs [9]. A numerical study of  $\text{As}_2\text{S}_3$  Raman fiber lasers was carried out to show their potential for the entire coverage of the  $3\text{--}4 \mu\text{m}$  spectral band [10]. Unfortunately, soft glass fibers have significant limitations

so far. They are often mechanically weak, and therefore require careful handling. Low-loss splicing with silica fiber is challenging, and their lower laser damage threshold makes power handling capability not comparable to that of conventional silica fibers.

Silica fiber is the best developed type of glass fiber, which is mechanically strong and has easy handling.  $\text{Tm}^{3+}$ - and  $\text{Ho}^{3+}$ -doped silica fiber lasers and amplifiers operate efficiently at  $1.9\text{--}2.1 \mu\text{m}$  wavelength range [11–14]. However, propagation loss of light increases steeply in silica fiber when wavelength is longer. Highly Ge-doped silica fibers have been used to generate  $>2.1 \mu\text{m}$  Raman lasers, because they have higher Raman gain coefficient and comparatively lower attenuation [15,16]. The longest wavelength reported so far by silica fiber Raman laser is  $2.41 \mu\text{m}$  with an output of  $24 \text{ mW}$ , which was achieved via spontaneous cascaded-Raman amplification [17].

Highly Ge-doped silica fiber can be easily spliced to usual silica fiber, which means that one can utilize available high-power  $2\text{-}\mu\text{m}$   $\text{Tm}^{3+}$ - or  $\text{Ho}^{3+}$ -doped fiber lasers as pump source to obtain  $2\text{-}\mu\text{m}$  Raman fiber lasers in an all fiber configuration. Since Raman gain is proportional to pump laser intensity, the high optical loss in silica-based fiber may be overcome with pulsed laser pumping. It is interesting and worthwhile to explore the long wavelength edge of silica fiber Raman laser operation.

In this paper, we investigate spontaneous cascaded Raman amplification in highly Ge-doped silica fiber at wavelengths far beyond  $2 \mu\text{m}$  with pulsed  $2\text{-}\mu\text{m}$  fiber laser as pump source. Numerical simulations are carried out first to verify the potential of high-efficiency 2nd-order Raman Stokes generation at wavelength longer than  $2.4 \mu\text{m}$ . In the experiments, when the pump laser is at  $2008 \text{ nm}$ , maximum 2nd Raman Stokes power of  $0.30 \text{ W}$  at  $2.43 \mu\text{m}$  is achieved with an optical efficiency of  $16.5\%$  and a peak power of  $275 \text{ W}$ . In the case of  $2040\text{-nm}$  pumping, maximum power of  $0.15 \text{ W}$  at  $2.48 \mu\text{m}$  is achieved with an optical efficiency of  $7.9\%$ . The results represent the longest wavelength operation of silica fiber lasers and the highest output Raman fiber laser at wavelength longer than  $2.4 \mu\text{m}$ .

In spontaneous cascaded Raman amplification process, spontaneous Raman emission is amplified by stimulated Raman scattering. The amplified Raman Stokes light excites

next Raman Stokes cascadedly. Normal dispersion fibers are usually desirable to avoid significant spectral broadening and to achieve efficient cascaded Raman conversion. The fiber investigated here is a highly Ge-doped step-index fiber (Nufern UHNA7), which has a core diameter of  $2.4\ \mu\text{m}$  and an NA of 0.41. Although the zero dispersion of fused silica is at  $1.3\ \mu\text{m}$ , UHNA7 fiber has a zero dispersion of  $\sim 2.6\ \mu\text{m}$  due to large normal waveguide dispersion.

Numerical simulations with simple model of coupled wave equations [18] are carried out to calculate the wavelength range that can be generated before the experiment. The most critical parameter in the simulation is the loss spectrum of the fiber. For wavelength  $< 2.4\ \mu\text{m}$ , the data are obtained from Ref. [17]. For wavelength  $> 2.4\ \mu\text{m}$ , the loss is estimated under the assumption of exponential growth with respect to wavelength. The resulted loss spectrum is shown in Fig. 1. At  $2.4\ \mu\text{m}$ , the loss is about  $700\ \text{dB/km}$ . At  $2.5\ \mu\text{m}$ , the loss increases to about  $4500\ \text{dB/km}$ . Figure 1 also plots calculated Raman gain as a function of wavelength at 0.5, 1, and 2 kW pumping that can be easily achieved in a pulse fiber laser. It is shown that the high loss can be easily overcome by pulsed laser pumping. The gain decreases with respect to wavelength due to the increasing mode area and the wavelength dependence of Raman gain coefficient.

Gaussian pulse is assumed in the laser simulation, and pulse width is set to  $100\ \text{ns}$ , which is close to the experimental condition. For nanosecond pulse and short fiber length (less than  $10\ \text{m}$  in the experiments), walk-off between the pump and laser pulses due to dispersion are negligible. Considering the optical damage threshold [19], the pulse peak power is limited up to  $5\ \text{kW}$  in the simulations. Since the fiber loss varies strongly with respect to wavelength and the Raman shift is constant as  $\sim 430\ \text{cm}^{-1}$ , the pump laser wavelength will influence the performance significantly. In the simulations, the pump source wavelength varies from  $1950$  to  $2150\ \text{nm}$ , which can be a  $\text{Tm}^{3+}$ - or  $\text{Ho}^{3+}$ -doped silica fiber laser. Then the 1st and 2nd Raman Stokes light will vary from  $2128$  to  $2369\ \text{nm}$  and  $2343$ – $2638\ \text{nm}$  accordingly.

Figure 2 shows the calculated conversion efficiencies of the 1st- and 2nd-order Stokes lights with optimized fiber length as functions of pump wavelength and pump peak power. It is found that with pump peak power of kW level, efficient 2nd Stokes Raman laser can be generated at wavelength longer than  $2.4\ \mu\text{m}$ . For example, if pump source has  $2\text{-kW}$  peak power at

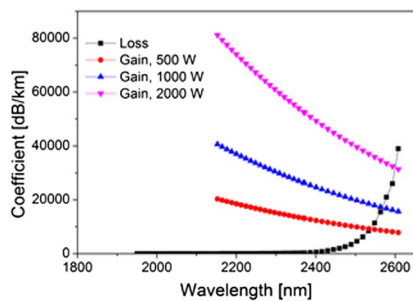


**Fig. 1.** Loss spectrum used in the simulation and calculated Raman gain ( $gP/A_{\text{eff}}$ ) as a function of wavelength at 0.5 kW, 1 kW, and 2 kW, respectively.

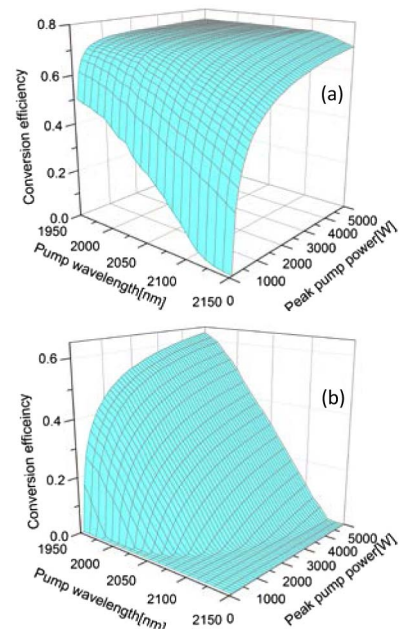


**Fig. 2.** Calculated conversion efficiency of (a) 1st and (b) 2nd Raman Stokes with different pump wavelength and peak pump power.

$2010\ \text{nm}$ ,  $2430\text{-nm}$  Stokes light can be generated with a conversion efficiency of 35%. If  $2\text{-kW}$  peak power  $2060\text{-nm}$  laser is chosen as pump source,  $2.5\text{-}\mu\text{m}$  Stokes light can be generated with a conversion efficiency of 15%. If pump peak power is as high as  $5\ \text{kW}$ , Raman Stokes light as long as  $2.6\ \mu\text{m}$  may be generated. The 3rd-order Stokes light cannot build up due to the huge fiber loss. The correctness of these predictions largely depends on the precision of fiber loss data used in the simulation.

The experimental setup consists of a  $2\text{-}\mu\text{m}$  actively  $Q$ -switched  $\text{Tm}$ -doped fiber seed laser, a  $2\text{-}\mu\text{m}$   $\text{Tm}$  fiber amplifier, and a piece of highly nonlinear Raman gain fiber (Nufern, UHNA7), as shown in Fig. 3. The  $2\text{-}\mu\text{m}$   $Q$ -switched seed source consists of a pair of  $2008\text{-nm}$  FBGs ( $2040\ \text{nm}$  in other set of experiments), a fiber-pigtailed multimode diode laser at  $793\ \text{nm}$ , a  $(2 + 1) \times 1$  combiner, a piece of  $3\text{-m}$   $\text{Tm}$ -doped double-clad single-mode fiber (Nufern, PM-TDF-10P/130-HE, cladding absorption of  $4.7\ \text{dB/m}$  at  $793\ \text{nm}$ ), and a fiber-pigtailed acousto-optic modulator (AOM). A homemade cladding pump light stripper (CPS) is spliced between the gain fiber and AOM to remove the residual pump light. At a repetition rate of  $8\ \text{kHz}$ , the max output power at  $2008\ \text{nm}$  is  $230\ \text{mW}$

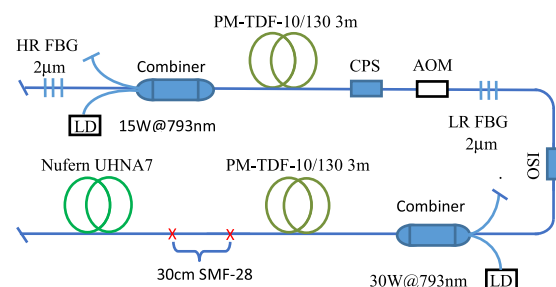


**Fig. 3.** Schematic experimental setup.

(237 mW at 2040 nm). A high-power broadband isolator is followed after the seed lasers to ensure that the seed laser is not affected by possible backward light from the amplifier. The loss caused by isolator is about 2 dB.

In the thulium-doped fiber power amplifier, the active fiber is a piece of 3-m Tm-doped double-clad fiber, the same as used in the seed laser. A high-power fiber-pigtailed diode laser at 793 nm with a maximum output power of 30 W is employed as the pump source. A piece of 0.3-m single-clad fiber (SMF-28) is spliced after the amplifier for stripping the residual 793-nm pump laser. With a 7-W incident pump power, the amplifier produces 1.82 W and 1.89 W average output power at 2008 and 2040 nm, respectively, at a repetition rate of 8 kHz. The output pulse width is about 100 ns, corresponding to peak power of 2.25 kW and 2.36 kW, respectively.

The silica-based UHNA7 fiber is directly fuse spliced to the single-mode SMF-28 fiber. The splice loss is  $\sim 0.5$  dB. So after the splice point, the pump peak power is reduced to about 2 kW. To find the optimal fiber length with the 2-kW pump peak power, the conversion efficiency of the Stokes light along the fiber is simulated. As shown in Fig. 4, the optimum fiber length is about 6 m for the 2nd Stokes light.

In the experiment, we have tested with 6- and 8-m-long UHNA7 fiber. The output spectra are analyzed with an optical spectrum analyzer (SM301-EX, Spectral Products), which has a resolution of 15 nm at 2-micron wavelength range. The power of the 2008-nm (residual pump), 2.20- $\mu\text{m}$  (1st Stokes), and 2.43- $\mu\text{m}$  (2nd Stokes) laser from the 6-m-long Raman fiber amplifier versus the 2008-nm incident pump power is plotted in Fig. 5(a). With 1.82-W incident pump power at 2008 nm, the total output is 0.85 W, of which 0.35 W and 0.30 W is at 2.20  $\mu\text{m}$  and 2.43  $\mu\text{m}$ , respectively. The corresponding optical efficiency from 2008 nm to 2.43  $\mu\text{m}$  is 16.5%. The conversion efficiency is only about half of the simulation result, which may result from the lower estimation of the fiber loss and broad spectrum of Raman emission. The output spectrum of the Raman fiber amplifier at maximum 2008-nm pump power is depicted in Fig. 5(b). Although the linewidth is broad, the Raman Stokes are clearly separated.

With a piece of 8-m UHNA7 fiber, the power ratios of 2.20  $\mu\text{m}$  and 2.43  $\mu\text{m}$  in the total output power are  $\sim 39.1\%$  and 43.2%, respectively. The fraction of 2.43- $\mu\text{m}$  laser increases. However, the total output power decreases to 0.635 W due to the higher loss of longer fiber. The 2.43- $\mu\text{m}$  laser decreases to 0.27 W instead, as shown in Fig. 5(a).

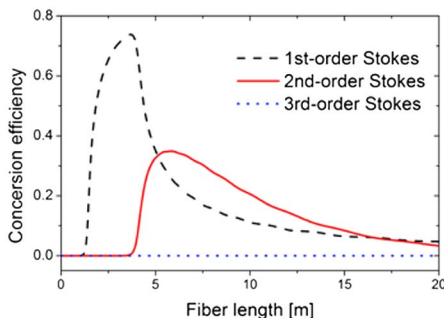


**Fig. 4.** Calculated conversion efficiency of the 1st and 2nd Stokes light with respect to the fiber length.

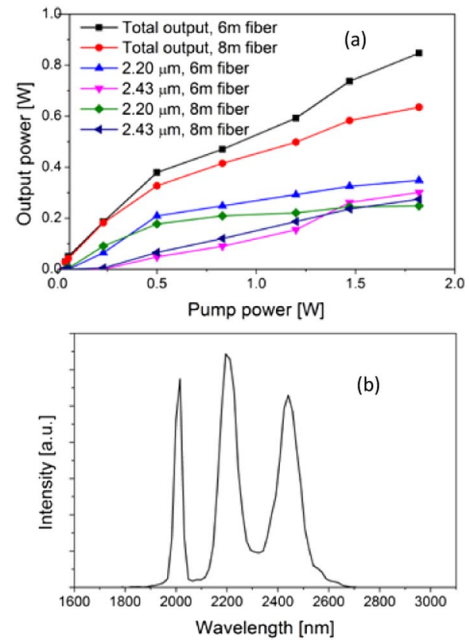


**Fig. 5.** (a) Output power of the 2.20- and 2.43- $\mu\text{m}$  Raman laser versus the 2008-nm incident pump power. (b) Output spectrum of the 6-m Raman fiber amplifier at maximum output.

For achieving longer wavelength output, the pump laser is switched to 2040 nm. At a repetition rate of 8 kHz, maximum average power is 1.89 W. So the incident pulse peak power is about 2.1 kW considering the 0.5-dB splice loss. The total output from the 6-m-long Raman fiber amplifier reaches 0.74 W. The output power and spectrum is depicted in Fig. 6. The power ratios of the 1st and 2nd Stokes at 2.24  $\mu\text{m}$  and 2.48  $\mu\text{m}$  are  $\sim 51.9\%$  and 20%, respectively. So the power of the 2.48- $\mu\text{m}$  Raman laser is calculated to be 0.15 W, which corresponds to a conversion efficiency of 7.9% from 2040 nm to 2.48  $\mu\text{m}$ . To the best of our knowledge, this is the longest wavelength ever reported for a silica-based fiber laser.

The temporal evolution of the laser pulse through the spontaneous cascaded Raman amplification process is also investigated. The measured pulse profile of the 2008-nm pump laser is seen in Fig. 7(a), while the pulse profile detected directly from the Raman amplifier is shown in Fig. 7(b), which contains 2008-nm, 2.20- and 2.43- $\mu\text{m}$  light. Figure 7(c) illustrates the

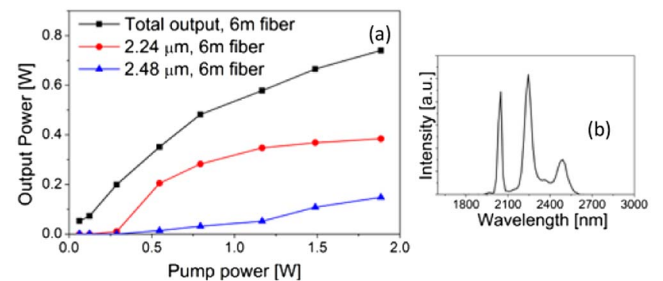


**Fig. 6.** (a) Output power of the 2.24- and 2.48- $\mu\text{m}$  laser from the 6-m Raman fiber amplifier versus the 2040-nm incident pump power. (b) Output spectrum of the Raman fiber amplifier at maximum output.

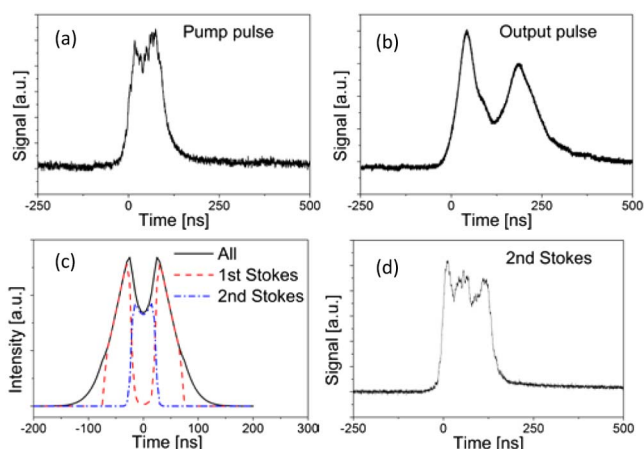


**Fig. 7.** (a) Measured pump laser pulse. (b) Measured amplifier output pulse. (c) Simulated pulse profiles for 1st and 2nd Stokes light, and complete Raman amplifier output. (d) Measured pulse of 2nd Stokes light at  $2.43\ \mu\text{m}$ .

simulated pulse profiles of complete Raman amplifier output, 1st and 2nd Stokes light with a 100-ns Gaussian pump pulse. The concave feature in the observed pulse is reproduced very well.

The central portion of the pump laser pulse is transferred from 2008 nm to  $2.20\ \mu\text{m}$  and  $2.43\ \mu\text{m}$  more efficiently, which results in a central dip. The pulse shape of 2nd-Stokes light (at  $2.43\ \mu\text{m}$ ) is measured with the help of a 500-nm band-pass filter centered at  $2.5\ \mu\text{m}$  (Thorlabs, FB2500-500). As shown in Fig. 7(d), the pulse has very sharp leading and trailing edges, as predicted in the simulation [Fig. 7(c)]. The pulse width is 137 ns, so the peak power at  $2.43\ \mu\text{m}$  is calculated to be 275 W. The pulses of Raman amplifier output are wider than the pump pulse. Nonlinear processes like self- and cross-phase modulation may contribute during the spontaneous cascaded Raman amplification process, which leads to the pulse broadening. We will investigate the phenomenon in the future experiment and simulation.

In conclusion, we have explored Raman laser generation at the long wavelength edge of silica fiber transmission. By two cascaded Raman conversion, 0.30 W at  $2.43\ \mu\text{m}$  is achieved with an optical efficiency of 16.5%, and a peak power of 275 W. 0.15 W at  $2.48\ \mu\text{m}$  is achieved with an optical

efficiency of 7.9%. The output wavelength obtained is currently the longest produced in silica fiber laser. We believe silica-based fiber Raman lasers have the potential to provide much higher output powers at wavelength as long as  $2.5\ \mu\text{m}$  with higher power pump source and optimal fiber length. In the future, we will work on further power scaling and wavelength extension of silica-based fiber Raman laser at mid-infrared spectral regime.

**Funding.** National Natural Science Foundation of China (NSFC) (61377062, 61378026).

## REFERENCES

1. S. D. Jackson, *Nat. Photonics* **6**, 423 (2012).
2. S. D. Jackson, *Opt. Lett.* **34**, 2327 (2009).
3. C. Carbonnier, H. Tobben, and U. B. Unrau, *Electron. Lett.* **34**, 893 (1998).
4. J. Schneider, C. Carbonnier, and U. B. Unrau, *Appl. Opt.* **36**, 8595 (1997).
5. A. Haboucha, V. Fortin, M. Bernier, J. Genest, Y. Messaddeq, and R. Vallee, *Opt. Lett.* **39**, 3294 (2014).
6. V. Fortin, M. Bernier, N. Caron, D. Faucher, M. E. Amraoui, Y. Messaddeq, and R. Vallee, *Opt. Eng.* **52**, 054202 (2013).
7. O. Henderson-Sapir, J. Munch, and D. J. Ottaway, *Opt. Lett.* **39**, 493 (2014).
8. V. Fortin, M. Bernier, D. Faucher, J. Carrier, and R. Vallee, *Opt. Express* **20**, 19412 (2012).
9. M. Bernier, V. Fortin, M. El Amraoui, Y. Messaddeq, and R. Vallee, *Opt. Lett.* **39**, 2052 (2014).
10. V. Fortin, M. Bernier, M. El-Amraoui, Y. Messaddeq, and R. Vallee, *IEEE Photon. J.* **5**, 1502309 (2013).
11. P. F. Moulton, G. A. Rines, E. V. Slobodtchikov, K. F. Wall, G. Frith, B. Samson, and A. L. G. Carter, *IEEE J. Sel. Top. Quantum Electron.* **15**, 85 (2009).
12. G. D. Goodno, L. D. Book, and J. E. Rothenberg, *Opt. Lett.* **34**, 1204 (2009).
13. K. Yin, B. Zhang, G. H. Xue, L. Li, and J. Hou, *Opt. Express* **22**, 19947 (2014).
14. N. Simakov, A. Hemming, W. A. Clarkson, J. Haub, and A. Carter, *Opt. Express* **21**, 28415 (2013).
15. E. M. Dianov, I. A. Bufetov, V. M. Mashinsky, V. B. Neustruev, O. I. Medvedkov, A. V. Shubin, M. A. Melkumov, A. N. Gur'yanov, V. F. Khopin, and M. V. Yashkov, *Quantum Electron.* **34**, 695 (2004).
16. J. Liu, F. Tan, H. Shi, and P. Wang, *Opt. Express* **22**, 28383 (2014).
17. P. T. Rakich, Y. Fink, and M. Soljačić, *Opt. Lett.* **33**, 1690 (2008).
18. G. P. Agrawal, *Nonlinear Fiber Optics* (Academic, 1997), Chap. 8.
19. D. J. Richardson, J. Nilsson, and W. A. Clarkson, *J. Opt. Soc. Am. B* **27**, B63 (2010).